EasyChair Preprint

№ 7925

Adhesion of the Metal and Composite Fiberglass Rebar with the Heavyweight Concrete

Oleksandr Chapiuk, Dmytro Oreshkin, Alina Hryshkova, Orest Pakholiuk and Irina Zadorozhnikova

May 5, 2022

Adhesion of the metal and composite fiberglass rebar with the heavyweight concrete

Chapiuk, O.[1[0000-0003-0283-1863]], Oreshkin, D.[2[0000-0003-0924-1903]], Hryshkova, A. [1[0000-0003-0432-4865]], Pakholiuk, O. [1[0000-0002-0650-6446]], Zadorozhnikova, I. [1[0000-0003-3652-7528]]

[1] Lutsk National Technical University, Lutsk, Ukraine
[2] LLC Technology Group "EKIPAZH, Kharkiv, Ukraine

Abstract. Since the adhesion of reinforcement to concrete is the main factor of their joint operation, and the studies of fiber-glass composite bars with concrete are obviously insufficient despite the growth in their use in road and housing construction, an analysis was conducted to compare the adhesion between metal and fiber-glass reinforcement with heavy-weight concrete by the beam method. The adhesion forces create a complex stress-strain condition in the concrete adjacent to reinforcement bars. Such condition results in distribution of stresses along the reinforcement axis, so that the longitudinal forces on the reinforcement become variable along the entire bar length. It has been experimentally proven that as the stress on the concrete beam is increasing in the areas of contact between the reinforcement and concrete, shear stresses are observed to be shifting from the starting points towards the end ones within the anchoring area; and for metal reinforcement, the shear stresses are less than for glass composite. It has been determined that the adhesion stress between glass-fiber reinforcement and concrete is significantly higher than steel reinforcement.

Keywords: metal reinforcement; fiber-glass composite reinforcement; heavy-weight concrete, adhesion between reinforcement and concrete; beam method RILEM-CEB-FIP; shear stresses; tension gauges.

1 Introduction

Year by year, the interest to using composite reinforcement in supporting construction designs of buildings and structures is growing. It is predetermined by its improved corrosion resistance, high tensile strength, viscoelasticity nature of relative elongation over the entire range of stresses, small values of elongation at rupture (0.5-3.0%), thermal expansion coefficient close to concrete, low specific gravity, high chemical resistance, including resistance to alkalis, as well as magnetic inertness, dielectric properties, radio transparency and low heat transfer coefficient (100 times less than steel) [1, 2]. FRP strength corresponds to the class steel reinforcement Am-IV, at the same time characterized by low modulus values (3.5 times), LTEC (2.5 times) and elongation (4-5 times) [3]. In the works [4, 5] it has been proved that for the metal

rebars with diameter of 16 mm the tangential stresses of the reinforcement and concrete bonding are 9.4% less than for the fiberglass reinforcement with diameter of 10 mm.

Despite the above advantages, composite reinforcement has some disadvantages: as compared to steel reinforcement, 4 times lower modulus of elasticity [6], brittleness at failure (absent fluidity limit), anisotropic properties of the material (low values of ultimate shear strength and axial compression), low fire resistance (up to 100 °C) and slight water absorption, which can lead to a loss of structures strength over time. To prevent water absorption, it is possible to treat composite rods with special substances, for example, "SILOL®" made in Ukraine, which also contributes to a significant increase in the adhesion of rods with concrete [7].

In most cases, glass-fiber and basalt composite reinforcement is used in erection (repair) of infrastructure facilities in road [8, 9], hydraulic engineering and geotechnical construction [10]: for reinforcement of slabs on distributed bases, basements of buildings and structures, as well as for reinforced concrete structures which are not subject to fire resistance requirements. To extend the scope of using composite reinforcement, it is conduct major studies and comparisons with the traditional metal reinforcement. In the researches [11, 12] it was found that the carrying capacity of beams with composite reinforcement (depending on the diameter of the rods) is 1.5 times higher and more than of beams with metal reinforcement. In almost all tests it was found that the outer shell of composite rebar works most efficiently, while the core - composite fibers - work within the limits of 10...15% by volume.

More and more scientists are currently dealing with issues of composite reinforcement functioning in flexural elements. Such research works may be divided into two groups: concrete elements reinforced exceptionally with composited fiberglass rebar FRP (AKC), and elements with combined reinforcement [13,14]. It has been carried out the comparison of the considered methods of calculation in USA, European Union, Russia and Ukraine and it has been defined that under-estimating of calculated resistance to tension of FRP that leads to inaccurate definition of fracture character of a bending element and construction over-reinforcing up to 50% [15, 16]. The improved methods of calculation are offered [17, 18, 19], that allows to estimate more accurately and reliably the fracture character of elements and to define breaking forces.

The adhesion between the reinforcement and concrete is an important property of reinforced concrete which determines its supporting capacity, rigidity and crack resistance, and it depends on a great number of factors, such as concrete strength, reinforcement type and diameter, the length of making bars into concrete, the nature of loads, hardening conditions, the location of bars during concreting, etc. Due to these, that at different parameters of die-rolled section [20-23] the composite reinforcement of different manufacturers will have different adhesion characteristics with concrete [24, 25].

The joint operation of composite rods with concrete is ensured by the adhesion of the cement with epoxide coating rather than by mechanical interlocking of the coils in the concrete matrix, as opposed to die-rolled section metal rods. The arrangement of

the die-rolled section by means of a sticking the impregnated binder bundle made of composite fibers is inexpedient, as this winding is cut from the surface of the rod at pulling, and the adhesion of concrete to the epoxy coating exceeds the cohesive strength of concrete and is sufficient to anchor the rods in it. It is more appropriate to die-roll the core itself by "crimping" it with a thin bundle in 1-2 steps of the core diameter. This increases the specific area of contact with concrete, improves the conditions of joint work of the composite with concrete under load, which will more fully realize the strength properties of the reinforcement when working in the supporting structure [26, 27].

The peculiarity of interaction between reinforcement and concrete is the presence of mutual displacements between them, resulting in a redistribution of forces. The areas in which the redistribution of forces is observed are called reinforcement anchoring zones. This issue is well known for reinforced concrete, but for composite reinforcement is almost not studied, despite its wide application in construction. It follows from the stated above that nowadays there is an urgent need for researches of composite reinforcement bonding with concrete and improvement of calculation methods and anchoring on the basis of experimental research results and comparison with metal reinforcement.

2 Methods

2.1 Structure of test specimens and their manufacturing materials

The experimental research program provides for the testing of three BMR beams (a beam with metal reinforcement of sickle profile) and three BCR (beam with glass-composite reinforcement manufactured by LLC "Ekibazh" Technology Group). Test beams with a total length of 1230 mm made of concrete class C20/25 of rectangular cross-sectional size 120x220 mm and consist of two halves that are connected in a stretched area by a reinforcing bar.

The diameters of the rebars are adopted based on the equal strength replacement of the rods. The ultimate tensile strength of the composite reinforcement AKC800 is almost twice stronger than metal reinforcement (tab. 1), thus it was decided to compare the adhesion with the concrete of Ø16A500C and Ø12AKC800, the adhesion area of which is twice smaller due to smaller length of anchorage 10d (160 mm - Ø16 A500C and 120 mm - Ø12AKC800).

Table 1. Comparative analysis of A500C and AKC800.

Material	Steel	Fiberglass
Ultimate tensile strength, σ, MPa	495	958
Modulus of elasticity, E, MPa	199	51
Relative elongation, %	8…25	1…3
Replacement of reinforcement (by strength)	16 A500C	12 AKC800
Weight of 1 linear meter, kg	16 A500C – 1.58	12 AKC800 – 0.169

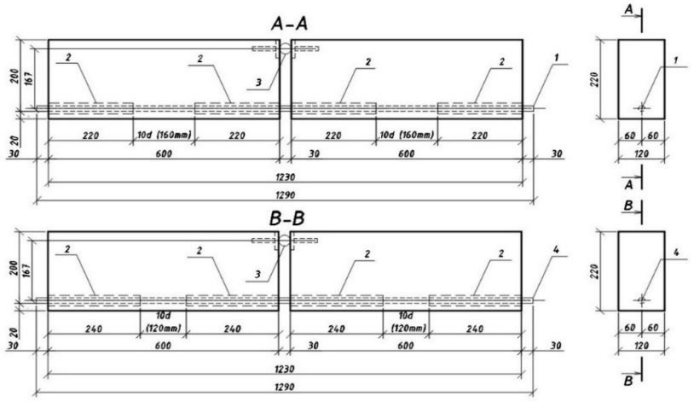

Fig. 3. Structure of test specimens – concrete beams BSR and BFR: 1 – steel reinforcement Ø16 A500C; 2 – plastic tube; 3 – steel cylinder; 4 – fiberglass composite reinforcement Ø12 AKC800.

In the compression area, a swivel joint was used in the form of two embedded parts with a steel cylinder between them. In each half of the beam, the bar had adhesion to the concrete at a length of 10d (d – bar diameter), whereas other areas were free of adhesion because the reinforcement bar was placed in plastic tubes with the length l (l = 220mm – for steel reinforcement Ø16 and l = 240 mm – for composite reinforcement Ø12) of each. In the compression area, the distance from the axis of the tested bar to the axis of the metal cylinder (lever arm) was 167 mm, the length of each half of the beam was 600 mm, the distance between the haves was 30 mm. The structure of the beams is given on Fig. 3. The reinforcement was fitted with tension gauges for studying the dynamics of tensions in the reinforcement bars.

2.2 Methods of Experimental Studies

The selection of samples and experimental studies of testing concrete beams were carried out using the RILEM/CEB/FIB beam method [28] for bending (Fig. 4a, Fig. 4b), since it is a generally accepted standard in most developed countries. This method consists in measuring the motions of free ends of the tested bars during the test procedure, and the measurements are recorded by means of dial indicators graduated in 0.001 mm located on the beam ends. The beams were stressed with two concentrated forces P1 (P/2), the distance between which was 400 mm.

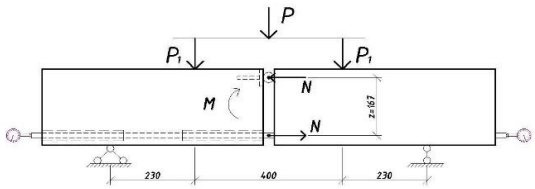

Fig. 4a. Design scheme for concrete beams.

Fig. 4b. General view for concrete beams.

The longitudinal strains of the bar embedded into the concrete were measured with resistance strain gauges in the beams at each stress stage. In the reinforcement bars of the test specimens, longitudinal grooves with the depth of 2 mm were symmetrically selected, and the resistance strain gauges were located in them to measure the bar strains during the flexural test of the concrete beam.

The resistance strain gauges were glued with epoxy glue BF2 and waterproofed with epoxy resin. Lead wired were set from the resistance strain gauges, and then the resistance strain gauges were connected to the tension gauge station.

3 Results and Discussion

3.1 Distribution of strains in adhesion between reinforcement and concrete in the test specimens BSR (feather-section bar A500C with steel reinforcement) and BFR (AKC800 with fiberglass composite reinforcement)

The destruction of all experimental twin beams occurred at fairly close loading values. Samples with BMR metal reinforcement were destroyed at 52.8; 54.0; 55.0 kN, and with glass composite reinforcement BSR at 44.0; 45.0; 46.2 kN. Further, the work shows the values of stresses at control points along the beams, which collapsed under medium loads.

When the specimen – concrete beam BSR – was tested by means of the resistance strain gauges, the strains of the reinforcement bar ε_{si} arising in the middle of the bar length, i.e. in the points i - 1, 2, 3, 4, 5, 6, 7, 8, 9 (Fig. 7) were measured.

The maximum value of the strain arising in the reinforcement bar f_{ydm}= 168.16 MPa was recorded in the middle under the stress close to the destroying value of P_u = 54 kN.

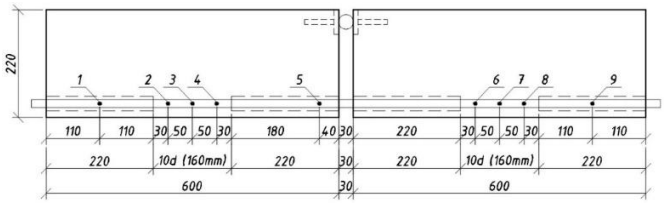

Fig. 7. Layout of the resistance strain gauges in the test specimen – concrete beam BSR.

It was more interesting to assess the distribution of tangential stresses in the reinforcement bars when in contact with concrete. For this purpose, the anchoring areas (10d in width) containing the points i - 2, 3, 4, 6, 7, 8 were examined in detail for BSR. These points divided the anchoring (concrete adhesion) areas of the bar into 9 zones. It was assumed that the force $f_{ydi}A_s$ affects each i^{th} zone of the bar, and then it is transferred to concrete due to emerging adhesion strains, as well as to the following bar zones (which concerns only the zones located within the anchoring areas). In such case, the tangential adhesion stresses in the middle of the zones τ_{mi} may be determined by the formula:

$$\tau_{mi} = \frac{(f_{ydi} - f_{yd,i-1}) \cdot A_s}{\pi d l_i} \quad (1)$$

where f_{ydi} and $f_{yd,i-1}$ are the strains in the bar in the i^{th} and previous zones;
A_s- the area of reinforcement;
l_i - the length of the i^{th} zone.
The mean tangential adhesion stresses between the reinforcement and concrete may be determined by the formula:

$$\tau_m = \frac{(f) \cdot A_s}{\pi d l} \quad (2)$$

where f – is the strain in the bar;
l - is the bar length.

Based on the determined mean tangential adhesion strains in each section, the curves of their distribution have been drawn along the length of anchorage of the reinforcement bar in concrete for different level of stresses, namely P = 5, 15, 25, 35, 45, 50 kN and under such destroying stress as P_u = 54 kN (Fig. 8).

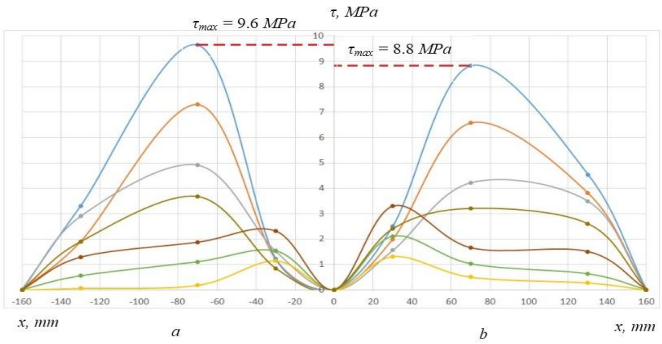

Fig. 8. Diagram of distribution of the tangential stresses in the zones of adhesion between the rod and concrete, depending on the stress P: a – adhesion area 1 in which the tension gauges 2, 3 and 4 are located, b – adhesion area 2 in which the tension gauges 6, 7 and 8 are located; – P = 5kN; – P = 15 kN; – P =25 kN; – P = 35 kN; – P = 45 kN; – P = 50 kN; – P_u = 54 kN (destroying force), τ_{max} – represents the maximum tangential adhesion strains between the reinforcement bar and concrete determined by the formula (2).

In the first adhesion zone (measured with the tension gauges 2, 3 and 4) at the first levels of stress P = 5 kN, P = 15 kN and P = 25 kN, the maximum strains emerged at the distance of x = 30 mm (4) from the starting point of the anchoring area, and they were equal τ = 1.14, 1.53 and 2.31 MPa, respectively. As the stresses increased, the maximum tangential adhesion strains grew in the points 3 and, to a lower extent, in 2. But under the stress of 35 kN (64% of the destroying value), the maximum tangential adhesion strains were already recorded at the point 3 where they were much higher than at the point 4. As the stressing forces was growing, the adhesion strains were increasing in point 3 and were gradually decreasing in the points 2 and 4, which indicated gradual destruction of the contact layer in those points, as well as pulling of the reinforcement out of the concrete body. When the beam BSR (P_u = 54 kN) was destroyed, the maximum adhesion strains reached their ultimate value τ_{max}= 9.6 MPa. The beam was definitely destroyed due to an insufficient length of bar anchorage, which was 10d. For the reinforcement to be broken, the necessary length of embedding should be at least 25d.

A similar pattern was also recorded in the first adhesion zone (with the tension gauges 6, 7, 8). Under the minimum stresses P = 5 kN, P = 15 kN and P = 25 kN, the maximum strains arose at the distance of x = 30 mm (6) from the starting point of the anchoring area, and they were τ = 0.60, 2.124 and 3.29 MPa respectively. The maximum tangential adhesion strains in the point 7 under the stress of 25 kN were twice lower than in the point 6, but when the stress was increasing up to 35 kN (64% of the destructive value), the tangential adhesion strains started lowering in the point 6 and increasing in the points 7 and 8, and in all these points it was equal to a lower value: τ = 3 MPa (35% of the maximum value). As the stresses were growing, the maximum tangential adhesion strains were increasing in the points 7 and 8, while they were lowering in the starting point of the anchoring area (6). Before the beam BSR was destroyed under the ultimate stress of P_u = 54 kN, the maximum adhesion strains between the reinforcement and concrete reaches the maximum value τ_{max}=8.8 MPa in the middle area of anchoring (8).

The analysis of each adhesion zone shows that as the stress on the beam BSR anchored with steel reinforcement Ø16 of the grade A500C is increasing, the tangential strains gradually move from the starting point of the anchoring area to its ends. Before the destruction, the maximum adhesion strains were τ_{max1}= 9.6 MPa in the left adhesion zone and τ_{max2}= 8.8 MPa in the right one.

Concerning the test specimen – the concrete beam BFR reinforced with fiberglass composite Ø12AKC800, its destruction strain was P = 45 kN, which was 17% less than the ultimate stress of the beam BSR.

To compare the stress-strain behavior in the test specimens – beams BSR and BFR, it is necessary to assess the distribution of the tangential strains in the composite reinforcement bar when in contact with concrete. For this purpose, the anchoring zones with a length of 10d containing the points i - 2, 3, 5, 6 were examined in detail. These points divided the anchoring (concrete adhesion) areas of the bar into 6 zones (see Fig. 9).

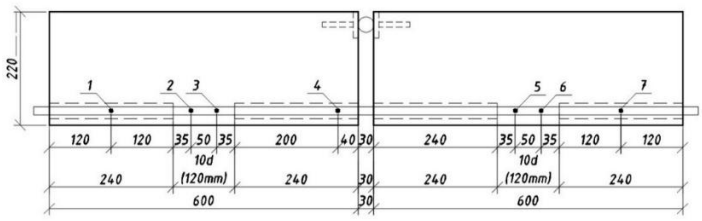

Fig. 9. Layout of resistance strain gauges in the specimen BFR.

Based on the determined mean tangential adhesion strains, the curves of their distribution along the length of anchorage of the reinforcement bar in concrete have been drawn in each zone for definite stress levels, namely P = 5, 15, 25, 35 kN, as well as for the destructive stress of P_u = 45 kN (Fig. 10).

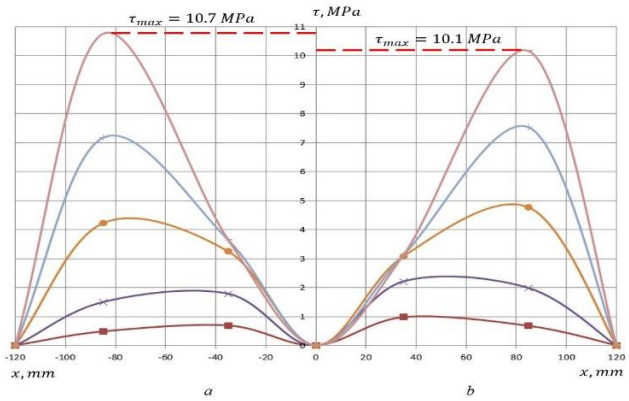

Fig. 10. Diagram of distribution of the tangential strains in the zones of adhesion between the bar and concrete, depending on the stress P: a – adhesion zone 1 in which the tension gauges 2 and 3 are located; b – adhesion section 2 in which the tension gauges 5 and 6 are located; – P = 5 kN; – P =15 kN; – P =25 kN; – P =35 kN; – P_u = 45 kN (destroying force), τ_{max}- maximum tangential adhesion stresses between the reinforcement bar and concrete determined by the formula (2).

In the first adhesion zone (with the tension gauges 2 and 3) (see Fig. 10, a), under the minimum level of stress P = 5 kN, the maximum stress emerged in the proximal anchoring point at the distance of 35 mm (3) where it was equal to τ = 0.69 MPa. Under the stress of P = 15 kN, the maximum strains were τ = 1.78 MPa. As the stresses were increasing up to the level of P = 25 kN, the maximum strain was already recorded in the distant point at the distance of 85 mm from the starting point of anchorage – in the point 2 where it was equal to τ = 4.21 MPa. Before the beam BFR was destroyed under the ultimate stress P_u = 45 kN, the maximum adhesion strains between the reinforcement and concrete reached their maximum value: τ_{max} = 10.7 MPa in the distant area of anchorage (2).

Analyzing the location of the curves on the graph showing the distribution of the tangential strains (see Fig.10, b) shows that the adhesion zone 2 (with the tension gauges 5 and 6) symmetrically reflects the adhesion zone 1. Under the minimum level of stress P = 5 kN, the maximum strain was recorded in the area of the 5 gauge where it was equal to τ = 0.98 MPa. As the force is increased up to P = 15 kN, the strains reach their maximum value τ = 2.21 MPa in the both gauges 5 and 6. The maximum strains are τ = 4.76 MPa under the strain of P = 25 kN, and under the ultimate strain of P_u = 45 kN the maximum adhesion strain between the reinforcement and concrete reached the maximum value of τ_{max}= 10.1 MPa in the distant area of anchorage (6) (tab. 2).

Table 2. Values of tangential adhesion strains τ, MPa of metal reinforcement Ø16A500C and Ø12AKC800 with concrete/

Stress level, kN	Tangential adhesion strain τ, MPa, between metal reinforcement Ø16A500C and concrete			Tangential adhesion strain τ, MPa, between composite reinforcement Ø12AKC800 and concrete		
	τ_{left}, MPa	τ_{right}, MPa	τ_{mean}, MPa	τ_{left}, MPa	τ_{right}, MPa	τ_{mean}, MPa
5	1.14	0.6	0.87	0.69	0.98	0.83
15	1.54	2.12	1.83	1.78	2.21	1.99
25	2.31	3.29	2.80	4.21	4.76	4.48
35	4.67	2.88	3.77	7.17	7.53	7.35
45	6.92	4.27	5.59	10.7	10.1	10.4
50	8.31	6.19	7.25			
55	9.60	8.80	9.20			

The graph shows the dependence of average values of the mean values of the maximum tangential adhesion strains between the reinforcement bars and concrete τ, MPa in the adhesion zones of the beams BSR and BFR on the strains in the reinforcement f_{yd}, MPa (Fig. 11).

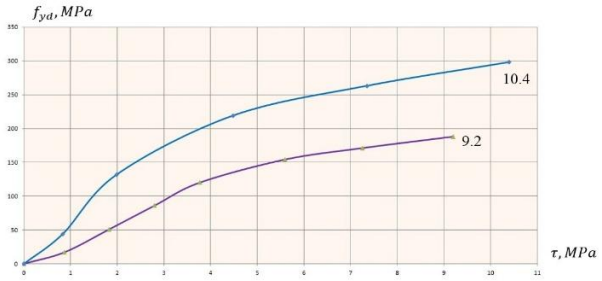

Fig. 11. Dependence of the mean value of the maximum tangential adhesion stresses between the reinforcement bars and concrete τ, MPa, of the adhesion zones of the beams BSR and BFR on the reinforcement f_{yd}, MPa, - Ø16A500C; - Ø10AKC800.

The curves of dependence of average values of maximum tangential tensions of rebar and concrete bonding from tensions in rebars have similar character. The maximum values are on average in metal rebar Ø16A500C - τ_c= 9.2 MPa, and in fiberglass rebar Ø10AKC800 - τ_c= 10.4 MPa, which is 11.5% higher.

3.2 Discussion

After analyzing each of the adhesion sections, it shows that with an increase in the load of a concrete beam in the areas of contact between reinforcement and concrete, the maximum values are on average in metal reinforcement Ø16A500C - τ_{max}= 9.2 MPa, and in fiberglass reinforcement Ø10AKC800 - τ_{max}= 10.4 MPa, which is 11.5% more.

With the anchoring length of 10d, the ultimate destroying strain in the beam BSR was equal to 54 kN, and in the beam BFR it was 45 kN. It is due to the fact that the anchoring length is 1.3 times longer, and the area of the contact layer of concrete with the metal rebar is 1.7 times larger than that of fiberglass rebar.

The graph in Fig. 11 shows that significant normal strains in composite reinforcement do not cause any increase in tangential strains. It is due to lower stress-strain properties of fiberglass composite reinforcement, although the maximum tangential adhesion strains with concrete are only 11.5% higher as compared to metal reinforcement.

4 Conclusions

1. The nature of distribution of tangential adhesion strains of both metal and fiberglass reinforcement with concrete is the same, and it is parabolic in form.
2. At maximum breaking loads in a concrete beam in the areas of reinforcement and concrete contact, the maximum stresses of metal reinforcement Ø16A500C are 11.5% less than for fiberglass rebar Ø12AKC800.
3. With a larger contact layer of concrete with metal ribbed rebar Ø16A500C in 1.7 times compared to fiberglass rebar Ø12AKC800 the maximum breaking load is only 17% higher.
4. Experimentally proved the possibility of equal replacement of metal rebar with fiberglass rebar of smaller diameter by the example of Ø16A500C and Ø12AKC800.

References

1. Safti, A., Benmokrahe, B., Rizkalla, S.: Degradation Assessment of Internal Continuous Fiber Reinforcement in Concrete Environment. Materials Reseach Report. University of Nort Florida. - UNF Projekt Contract No. BDK 82 # 977 – 05. P. 398 (2013).
2. Plevkov, V., Baldin, I., Kudyakov, K., Nevskii, A.: Mechanical properties of composite rebar under static and short-term dynamic loading AIP Conference Proceedings 1800, 040018 (2017).

3. Avdeeva, A., Shlykova, I., Antonova, M., Barabanschikov, Y., Belyaeva, S.: Reinforcement of concrete structures by fiberglass rods. MATEC Web of Conferences 2016, pp. 1-5 (2016).
4. Chapiuk, O., Hryshkova, A., Kysliuk, D., Zadorozhnikova, I., Pakholiuk, O.: Zcheplennia metalevykh ta kompozytnykh sterzhniv z vazhkym betonom [Assembly of metal and composite steel with hard concrete]. Suchasni tekhnolohii ta metody rozrakhunkiv u budivnytstvi. Pp. 186-194. Lutsk National Technical University, Lutsk (2018).
5. Chapiuk, O., Kysliuk, D., Hryshkova, A.: Doslidzhennia dotychnykh napruzhen zcheplennia sklokompozytnykh ta metalevykh armaturnykh sterzhniv z vazhkym betonom [Research of tactical tensions of clutch of glasscomposite and metal reinforcement bars with heavy concrete]. Resursoekonomni materialy, konstruktsii, budivli ta sporudy. Pp. 240-247. Rivne (2019).
6. Seo, D., Park, K., Kim, H.: Enhancement in Elastic Modulus of GFRP Bars by Material Hybridization. Pp. 865-869. Engineering (2013).
7. Chapiuk, O., Olekh, V., Orieshkin, D.: Zcheplennia vazhkoho betonu z kompozytnoiu skloplastykovoiu armaturoiu, pokrytoiu hidroizoliatsiinoiu kompozytsiieiu SILOL® [Adhesion of heavy concrete with composite fiber fixtures coated with SILOL® waterproofing composition]. Suchasni tekhnolohii ta metody rozrakhunkiv. Zbirnyk FBD. Pp. 253-262. Lutsk National Technical University, Lutsk (2017).
8. Solodkyy, S., Koval, P., Babiak, I., Hrymak, O.: The impact of basaltic fiber on characteristics road concretes. Ibausil 19 Internationale Baustofftagung, pp. 1067-1074. Weimar Bundesrepublik Deutschland (2015).
9. Koval, P., Hrymak, O.: Vplyv malotsyklovykh navantazhen na robotu betonnykh balok, armovanykh bazaltoplastykovoiu armaturoiu [Consideration of the effect of low-cycle loads on bended concrete beams reinforced with basalt-plastic armature]. Mosty i tuneli: teoriia, doslidzhennia, praktyka. Pp. 8232-8236. Lviv (2017).
10. Weber, A., Juette, B.: GFRP – Reinforcement ComBAR® in Diaphragm Walls for the Construction of Subway and Sewer Tunnels. Proceedings CCC, P. 881 (2005).
11. Kustikova, Y.: Investigation of Basalt Plastic Reinforcement and Its Adhesion With Concrete. Construction: Science and Education. 2014. 1.
12. Gudonis, E., Kacianauskas, R., Gribniak, V., Weber, A., Jakubovskis, R., Kaklauskas, G.: Mechanical properties of the bond between GFRP reinforcing bars and concrete. Mechanics of composite materials. Pp. 641-654 (2014).
13. Hossain, K., Ametrano, D., Lachemi, M.: Bond Strength of GFRP Bars in Ultra-High Strength Concrete Using RILEM Beam Tests. Journal of Building Engineering. Pp. 69–79 (2017).
14. Castillo, E., Scott, R., Smith, T., Griffith, M.: Design approach for FRP spike anchors in FRP-strengthened RC structures Composite Structures. Pp. 23-33 (2019).
15. Kassem, C., Farghaly, A., Benmokrane, B.: Evaluation of Flexural Behavior and Serviceability Performance of Concrete Beams Reinforced with FRP Bars. Journal of Composites for Construction. Pp. 682-695 (2011).
16. Klimov, Yu., Soldatchenko, O., Oreshkin, D.: E`ksperimentalnye issledovaniya sczepleniya kompozitnoj nemetallicheskoj armatury s betonom [Experimental research of adhesion glass-fiber reinforcement with concrete]. URL: http://www.frp-rebar.com/frp-rebar_test_adhesion_concrete.html (2010).
17. Antakov, A., Antakov, I.: Sovershenstvovanie metodiki rascheta normalnykh sechenij izgibaemykh elementov s polimerkompozitnoj armaturoj [Improving the calculation method of normal section of bent elements with polymer-composite reinforcement]. Izvestiya KGASU. Pp. 154–160 (2015).

18. Begunova, N., Grahov, V., Vozmishchev, V., Kislyakova, I.: Comparative evaluation of results on test of concrete beams with fiberglass rebar and calculated data. Science & Technique. Pp. 155–163 (2019).
19. Baena, L., Torres, A., Turon, C.: Experimental study of bond behavior between concrete and FBP bars using a pull-out test. Composites. Pp. 784-797 (2009).
20. ACI 440 1R-15, Guide for the Design and Construction of Structural Concrete Reinforced with Fiber-Reinforced Polymer (FRP) Bars, American Concrete Institute (ACI) (2015).
21. CAN/CSA-S6-02. Design and Construction of Building Components with Fibre Reinforced Polymers. CSA, Canada (2002).
22. CNR-DT 203/2006. Istruzioni per la Progettazione, l'Esecuzione e il Controllo di Strutture di Calcestruzzo armato con Barre di Materiale Composito Fibrorinforzato (2006).
23. Recommendation for Design and Construction of Concrete Structures Using Continuous Fiber Reinforcing Materials. JSCE. 23 (1997).
24. Cosenza, G., Manfredi, R., Realfonzo R.: Behavior and Modeling of FRP Rebars to Concrete. Journal of composites for construction, pp. 40-51 (1997).
25. Ochola, R., Marcus, K., Nurick, G., Franz, T.: Mechanical behaviour of glass and carbon fibre reinforced composites at varying strain rates. Composite Structures. Pp. 455–467 (2004).
26. Khozin, V., Piskunov, A., Gizdatullin, A., Kuklin, A.: Sczeplenie polimerkompozitnoj armatury s czementnym betonom [Adhesion of polymer composite reinforcement with cement concrete]. Izvestiya KGASU. Pp. 214-220 (2013).
27. Gizdatullin, A., Khozin, V., Kuklin, A., Khusnutdinov, A.: Specifics of testing and fracture behavior of fibre-reinforced polymer bars. Magazine of Civil Engineering, pp. 40-47 (2014).
28. RILEM/CEB/FIP Recommendations RC 5: Bond test for reinforcing steel, 1. Beam Test (1978).